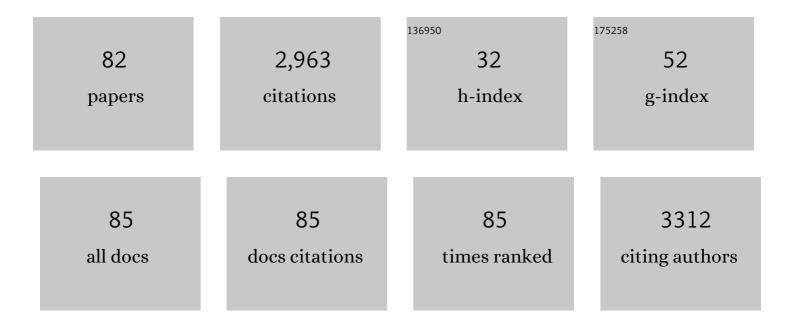
List of Publications by Year in descending order

Source: https://exaly.com/author-pdf/8514538/publications.pdf Version: 2024-02-01



PHODDI LEDVIS

#	Article	IF	CITATIONS
1	Machine learning as an online diagnostic tool for proton exchange membrane fuel cells. Current Opinion in Electrochemistry, 2022, 31, 100867.	4.8	16
2	Spatially Resolved Operando Synchrotron-Based X-Ray Diffraction Measurements of Ni-Rich Cathodes for Li-Ion Batteries. Frontiers in Chemical Engineering, 2022, 3, .	2.7	9
3	Dualâ€Metal Atom Electrocatalysts: Theory, Synthesis, Characterization, and Applications (Adv. Energy) Tj ETQq1	1,0.7843 19.5	14 rgBT /O
4	Thermal Runaway of Li-Ion Cells: How Internal Dynamics, Mass Ejection, and Heat Vary with Cell Geometry and Abuse Type. Journal of the Electrochemical Society, 2022, 169, 020526.	2.9	11
5	The effect of non-uniform compression on the performance of polymer electrolyte fuel cells. Journal of Power Sources, 2022, 521, 230973.	7.8	10
6	The effect of cell geometry and trigger method on the risks associated with thermal runaway of lithium-ion batteries. Journal of Power Sources, 2022, 524, 230645.	7.8	28
7	Efficient harvesting and storage of solar energy of an all-vanadium solar redox flow battery with a MoS <sub>2</sub> @TiO <sub>2</sub> photoelectrode. Journal of Materials Chemistry A, 2022, 10, 10484-10492.	10.3	11
8	Dualâ€Metal Atom Electrocatalysts: Theory, Synthesis, Characterization, and Applications. Advanced Energy Materials, 2022, 12, .	19.5	78
9	A greyscale erosion algorithm for tomography (GREAT) to rapidly detect battery particle defects. Npj Materials Degradation, 2022, 6, .	5.8	3
10	New strategies for interrogation of redox flow batteries via Synchrotron radiation. Current Opinion in Chemical Engineering, 2022, 37, 100836.	7.8	6
11	Correlative electrochemical acoustic time-of-flight spectroscopy and X-ray imaging to monitor the performance of single-crystal and polycrystalline NMC811/Gr lithium-ion batteries. Journal of Power Sources, 2022, 542, 231775.	7.8	5
12	Electrospinning as a route to advanced carbon fibre materials for selected low-temperature electrochemical devices: A review. Journal of Energy Chemistry, 2021, 59, 492-529.	12.9	56
13	Fabrication of high surface area ribbon electrodes for use in redox flow batteries via coaxial electrospinning. Journal of Energy Storage, 2021, 33, 102079.	8.1	21
14	<i>Operando</i> Bragg Coherent Diffraction Imaging of LiNi <sub>0.8</sub> Mn <sub>0.1</sub> Co <sub>0.1</sub> O <sub>2</sub> Primary Particles within Commercially Printed NMC811 Electrode Sheets. ACS Nano, 2021, 15, 1321-1330.	14.6	23
15	Towards a mechanistic understanding of particle shrinkage during biomass pyrolysis via synchrotron X-ray microtomography and in-situ radiography. Scientific Reports, 2021, 11, 2656.	3.3	10
16	A Dilatometric Study of Graphite Electrodes during Cycling with X-ray Computed Tomography. Journal of the Electrochemical Society, 2021, 168, 010507.	2.9	38
17	3D X-Ray Characterization of Energy Storage and Conversion Devices. , 2021, , 513-544.		Ο
18	2021 roadmap on lithium sulfur batteries. JPhys Energy, 2021, 3, 031501.	5.3	74

#	Article	IF	CITATIONS
19	Developments in Dilatometry for Characterisation of Electrochemical Devices. Batteries and Supercaps, 2021, 4, 1378-1396.	4.7	12
20	Highâ€Đensity Ligninâ€Đerived Carbon Nanofiber Supercapacitors with Enhanced Volumetric Energy Density. Advanced Science, 2021, 8, e2100016.	11.2	42
21	A novel fuel cell design for operando energy-dispersive x-ray absorption measurements. Journal of Physics Condensed Matter, 2021, 33, 314002.	1.8	6
22	Is lithium the key for nitrogen electroreduction?. Science, 2021, 372, 1149-1150.	12.6	37
23	Open-circuit dissolution of platinum from the cathode in polymer electrolyte membrane water electrolysers. Journal of Power Sources, 2021, 498, 229937.	7.8	9
24	Developments in Dilatometry for Characterisation of Electrochemical Devices. Batteries and Supercaps, 2021, 4, 1376-1377.	4.7	0
25	Characterizing Batteries by In Situ Electrochemical Atomic Force Microscopy: A Critical Review. Advanced Energy Materials, 2021, 11, 2101518.	19.5	40
26	Dendrite suppression by anode polishing in zinc-ion batteries. Journal of Materials Chemistry A, 2021, 9, 15355-15362.	10.3	41
27	Nanoscale state-of-charge heterogeneities within polycrystalline nickel-rich layered oxide cathode materials. Cell Reports Physical Science, 2021, 2, 100647.	5.6	12
28	Lignin-derived electrospun freestanding carbons as alternative electrodes for redox flow batteries. Carbon, 2020, 157, 847-856.	10.3	37
29	3D Carbon Materials for Efficient Oxygen and Hydrogen Electrocatalysis. Advanced Energy Materials, 2020, 10, 1902494.	19.5	97
30	Operando Electrochemical Atomic Force Microscopy of Solid–Electrolyte Interphase Formation on Graphite Anodes: The Evolution of SEI Morphology and Mechanical Properties. ACS Applied Materials & Interfaces, 2020, 12, 35132-35141.	8.0	65
31	Using In-Situ Laboratory and Synchrotron-Based X-ray Diffraction for Lithium-Ion Batteries Characterization: A Review on Recent Developments. Condensed Matter, 2020, 5, 75.	1.8	37
32	Data for an Advanced Microstructural and Electrochemical Datasheet on 18650 Li-ion Batteries with Nickel-Rich NMC811 Cathodes and Graphite-Silicon Anodes. Data in Brief, 2020, 32, 106033.	1.0	11
33	Identifying the Origins of Microstructural Defects Such as Cracking within Niâ€Rich NMC811 Cathode Particles for Lithiumâ€lon Batteries. Advanced Energy Materials, 2020, 10, 2002655.	19.5	119
34	Rapid Preparation of Geometrically Optimal Battery Electrode Samples for Nano Scale X-ray Characterisation. Journal of the Electrochemical Society, 2020, 167, 060512.	2.9	7
35	X-ray Micro-Computed Tomography of Polymer Electrolyte Fuel Cells: What is the Representative Elementary Area?. Journal of the Electrochemical Society, 2020, 167, 013545.	2.9	30
36	Correlative acoustic time-of-flight spectroscopy and X-ray imaging to investigate gas-induced delamination in lithium-ion pouch cells during thermal runaway. Journal of Power Sources, 2020, 470, 228039.	7.8	30

#	Article	IF	CITATIONS
37	Exploring cycling induced crystallographic change in NMC with X-ray diffraction computed tomography. Physical Chemistry Chemical Physics, 2020, 22, 17814-17823.	2.8	28
38	Theoretical transmissions for X-ray computed tomography studies of lithium-ion battery cathodes. Materials and Design, 2020, 191, 108585.	7.0	9
39	Electrocatalysis: 3D Carbon Materials for Efficient Oxygen and Hydrogen Electrocatalysis (Adv.) Tj ETQq1 1 0.784	314 rgBT 19.5	/Overlock 1
40	Probing the Structure-Performance Relationship of Lithium-Ion Battery Cathodes Using Pore-Networks Extracted from Three-Phase Tomograms. Journal of the Electrochemical Society, 2020, 167, 040528.	2.9	17
41	Realising the electrochemical stability of graphene: scalable synthesis of an ultra-durable platinum catalyst for the oxygen reduction reaction. Nanoscale, 2020, 12, 16113-16122.	5.6	11
42	Spatial dynamics of lithiation and lithium plating during high-rate operation of graphite electrodes. Energy and Environmental Science, 2020, 13, 2570-2584.	30.8	124
43	Resolving Liâ€lon Battery Electrode Particles Using Rapid Labâ€Based Xâ€Ray Nanoâ€Computed Tomography for Highâ€Throughput Quantification. Advanced Science, 2020, 7, 2000362.	11.2	26
44	Data on the theoretical X-Ray attenuation and transmissions for lithium-ion battery cathodes. Data in Brief, 2020, 30, 105539.	1.0	1
45	An Advanced Microstructural and Electrochemical Datasheet on 18650 Li-Ion Batteries with Nickel-Rich NMC811 Cathodes and Graphite-Silicon Anodes. Journal of the Electrochemical Society, 2020, 167, 140530.	2.9	39
46	Tailoring Carbon Nanotube Microsphere Architectures with Controlled Porosity. Advanced Functional Materials, 2019, 29, 1903983.	14.9	15
47	Representative resolution analysis for X-ray CT: A Solid oxide fuel cell case study. Chemical Engineering Science: X, 2019, 4, 100043.	1.5	2
48	Free-standing supercapacitors from Kraft lignin nanofibers with remarkable volumetric energy density. Chemical Science, 2019, 10, 2980-2988.	7.4	88
49	The effect of non-uniform compression and flow-field arrangements on membrane electrode assemblies - X-ray computed tomography characterisation and effective parameter determination. Journal of Power Sources, 2019, 426, 97-110.	7.8	46
50	Modelling and experiments to identify high-risk failure scenarios for testing the safety of lithium-ion cells. Journal of Power Sources, 2019, 417, 29-41.	7.8	93
51	Examining the effect of the secondary flow-field on polymer electrolyte fuel cells using X-ray computed radiography and computational modelling. International Journal of Hydrogen Energy, 2019, 44, 1139-1150.	7.1	15
52	Mass transfer in fibrous media with varying anisotropy for flow battery electrodes: Direct numerical simulations with 3D X-ray computed tomography. Chemical Engineering Science, 2019, 196, 104-115.	3.8	79
53	PoreSpy: A Python Toolkit for Quantitative Analysis of Porous Media Images. Journal of Open Source Software, 2019, 4, 1296.	4.6	184
54	Flow Batteries: Insights into the Effect of Structural Heterogeneity in Carbonized Electrospun Fibrous Mats for Flow Battery Electrodes by Xâ€Ray Tomography (Small 9/2018). Small, 2018, 14, 1870040.	10.0	2

#	Article	IF	CITATIONS
55	In situ compression and X-ray computed tomography of flow battery electrodes. Journal of Energy Chemistry, 2018, 27, 1353-1361.	12.9	42

56 Thermal Runaway: Identifying the Cause of Rupture of Liâ€lon Batteries during Thermal Runaway (Adv.) Tj ETQq0 0 0 rgBT /Overlock 10

57	Insights into the Effect of Structural Heterogeneity in Carbonized Electrospun Fibrous Mats for Flow Battery Electrodes by Xâ€Ray Tomography. Small, 2018, 14, 1703616.	10.0	31
58	Identifying the Cause of Rupture of Liâ€lon Batteries during Thermal Runaway. Advanced Science, 2018, 5, 1700369.	11.2	89
59	Xâ€ray Nano Computed Tomography of Electrospun Fibrous Mats as Flow Battery Electrodes. Energy Technology, 2018, 6, 2488-2500.	3.8	23
60	Multiscale tomographic analysis of the thermal failure of Na-Ion batteries. Journal of Power Sources, 2018, 400, 360-368.	7.8	7
61	Alkaline anion exchange membrane degradation as a function of humidity measured using the quartz crystal microbalance. International Journal of Hydrogen Energy, 2017, 42, 6243-6249.	7.1	13
62	Investigation of Hot Pressed Polymer Electrolyte Fuel Cell Assemblies via X-ray Computed Tomography. Electrochimica Acta, 2017, 242, 125-136.	5.2	74
63	A novel molten-salt electrochemical cell for investigatingÂthe reduction of uranium dioxide to uranium metal by lithium using <i>in situ</i> synchrotron radiation. Journal of Synchrotron Radiation, 2017, 24, 439-444.	2.4	6
64	Characterising thermal runaway within lithium-ion cells by inducing and monitoring internal short circuits. Energy and Environmental Science, 2017, 10, 1377-1388.	30.8	194
65	Fluid Transport Properties from 3D Tomographic Images of Electrospun Carbon Electrodes for Flow Batteries. ECS Transactions, 2017, 77, 129-143.	0.5	13
66	Tracking Internal Temperature and Structural Dynamics during Nail Penetration of Lithium-Ion Cells. Journal of the Electrochemical Society, 2017, 164, A3285-A3291.	2.9	102
67	The Importance of Using Alkaline Ionomer Binders for Screening Electrocatalysts in Alkaline Electrolyte. Journal of the Electrochemical Society, 2017, 164, F1551-F1555.	2.9	21
68	3D Printing: 3Dâ€Printed Structural Pseudocapacitors (Adv. Mater. Technol. 9/2016). Advanced Materials Technologies, 2016, 1, .	5.8	1
69	Design of a miniature flow cell for <i>in situ</i> x-ray imaging of redox flow batteries. Journal Physics D: Applied Physics, 2016, 49, 434002.	2.8	35
70	3Dâ€Printed Structural Pseudocapacitors. Advanced Materials Technologies, 2016, 1, 1600167.	5.8	32
71	Effect of gas diffusion layer properties on water distribution across air-cooled, open-cathode polymer electrolyte fuel cells: A combined ex-situ X-ray tomography and in-operando neutron imaging study. Electrochimica Acta, 2016, 211, 478-487.	5.2	78
72	The effect of felt compression on the performance and pressure drop of all-vanadium redox flow batteries. Journal of Energy Storage, 2016, 8, 91-98.	8.1	67

#	Article	IF	CITATIONS
73	The Hydro-electro-thermal Performance of Air-cooled, Open-cathode Polymer Electrolyte Fuel Cells: Combined Localised Current Density, Temperature and Water Mapping. Electrochimica Acta, 2015, 180, 307-315.	5.2	47
74	Investigating the effect of thermal gradients on stress in solid oxide fuel cell anodes using combined synchrotron radiation and thermal imaging. Journal of Power Sources, 2015, 288, 473-481.	7.8	33
75	Graphitic Carbon Nitride Materials for Energy Applications. ECS Transactions, 2015, 64, 13-30.	0.5	6
76	Following the electroreduction of uranium dioxide to uranium in LiCl–KCl eutectic in situ using synchrotron radiation. Journal of Nuclear Materials, 2015, 464, 256-262.	2.7	13
77	Mechanisms and effects of mechanical compression and dimensional change in polymer electrolyte fuel cells – A review. Journal of Power Sources, 2015, 284, 305-320.	7.8	76
78	Hydrogen Oxidation on PdIr/C Catalysts in Alkaline Media. Journal of the Electrochemical Society, 2014, 161, F458-F463.	2.9	46
79	Graphitic Carbon Nitride Supported Catalysts for Polymer Electrolyte Fuel Cells. Journal of Physical Chemistry C, 2014, 118, 6831-6838.	3.1	63
80	A novel high-temperature furnace for combined <i>inÂsitu</i> synchrotron X-ray diffraction and infrared thermal imaging to investigate the effects of thermal gradients upon the structure of ceramic materials. Journal of Synchrotron Radiation, 2014, 21, 1134-1139.	2.4	9
81	Novel PdIr/C Catalysts for the Hydrogen Oxidation Reaction in Alkaline Media. ECS Transactions, 2013, 58, 637-650.	0.5	3
82	Development of Graphitic-Carbon Nitride Materials as Catalyst Supports for Polymer Electrolyte Fuel Cells. ECS Transactions, 2013, 58, 1767-1778.	0.5	11